MRI SOLUTIONS

November 11, 2015

Dr. Andrew Rawicz
School of Engineering Science
Simon Fraser University
Burnaby, British Columbia
V5A 1S6

RE: ENSC 305W/440 Design Specification for a **Portable Magnetic Resonance Imaging Scanner**

Dear Dr. Rawicz,

The attached document contains the design specification for Portable Magnetic Resonance Imaging (MRI) Scanner. Our goal is to design a cost effective and portable MRI Scanner using simplified hardware and a projection-based imaging technique.

This design document describes the hardware and software implementation for a proof-of-concept model, focussing on the technical details and scientific background underlying the design choices. A test plan is also presented for future evaluation of the hardware and software components.

MRI Solutions consists of 5 determined, brilliant and compassionate senior engineering students: Anterpal Singh Sandhu, Barry Yim, Evangeline Yee, Gagandeep Kaur, and Robin Wisniewski. If you have any questions or concerns regarding this document, please do not hesitate to contact our Chief Communication Officer Gagandeep Kaur by email at gkaur@sfu.ca.

Sincerely,

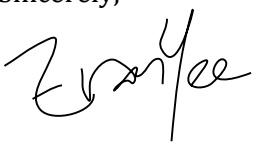

Evangeline Yee
CEO
MRI Solutions Inc.

Enclosure: Design Specification for a Portable Magnetic Resonance Imaging Scanner

Portable MRI Scanner

by

MRI SOLUTIONS

Project Team: Anterpal Singh Sandhu
Barry Yim
Evangeline Yee
Gagandeep Kaur
Robin Wisniewski

Contact Person: Gagandeep Kaur
gkaur@sfu.ca

Submitted to: Dr. Andrew Rawicz – ENSC 440
Steve Whitmore – ENSC 305
School of Engineering Science
Simon Fraser University

Issued Date: November 12, 2015
Revision Number: 1.0

Abstract

This document describes the design specifications for a portable MRI. MRI Solutions has devised a cost-effective and portable scanner that combines permanent magnet, radiofrequency and a computer to produce detailed images of bone and soft-tissue. Our unique approach utilizes the inherent inhomogeneity of permanent magnet for spatial encoding. The main hardware and software components are listed below:

- Magnet system
- Radiofrequency system
- Field Programmable Gate Array (FPGA) Control Centre
- Signal processing system

In this document, we describe the design considerations for each hardware and software component at different development stages. The design choices are presented with additional focus on the technical details and scientific background underlying the design choices. Justifications are made for the design approach chosen to ensure that the design specifications will meet the functional requirements.

A detailed test plan is also presented for future evaluation of the hardware and software components. This test plan describes the procedure to test the functionality of each component. The success of this project will be measured against this test plan.

Table of Contents

List of Figures and Tables

Glossary

MRI	:	Magnetic Resonance Imaging
Larmor Frequency	:	Rate of precession of the magnetic moment of the protons around the external magnetic field
Precession	:	A change in rotational axis of a rotating body
Halbach	:	An arrangement of permanent magnets which produces uniform magnetic field inside, with no magnetic field outside
RF	:	Radio Frequency
TR	:	Transmit Receiver
Spin Echo Pulse	:	In magnetic resonance, a spin echo is the refocusing of spin magnetisation by a pulse of resonant electromagnetic radiation. Modern nuclear magnetic resonance and magnetic resonance imaging make use of this effect.
FPGA	:	Field programmable gate array; An integrated circuit designed to be programmed by the user
DDS	:	Direct Digital Synthesizer
DAC	:	Digital to Analog Converter
ADC	:	Analog to Digital Converter
LNA	:	Low Noise Amplifier; An amplifier used to amplify weak signals without adding noise

1. Introduction

Our MRI scanner is an innovative solution to provide tissue and bone imaging. Designed to be cost-effective and portable, our MRI scanner will provide greater access to MRI scans and allow for remote imaging. The proposed design uses rotation of the magnet's inhomogeneous magnetic field and a projection-based imaging technique to reconstruct the spatial location of detected signals.

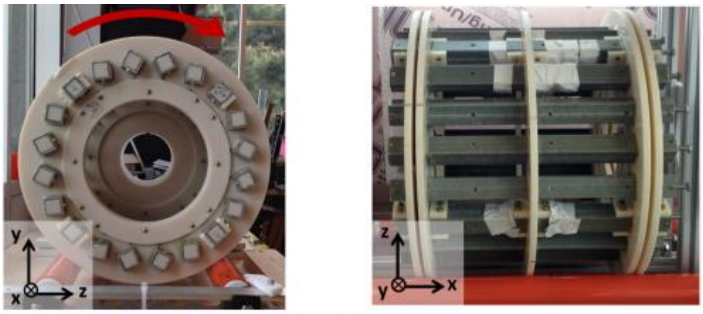

Figure 1: Projection-based imaging. Encode image by rotating magnet around the sample[1]

1.1 Background

Conventional MRI machines use strong magnetic fields to magnetize hydrogen protons in the human body. A radiofrequency pulse is then used to excite the protons. When the radiofrequency pulse is turned off, the hydrogen protons emit a response. This signal can be encoded to produce high quality images. To encode the spatial location of the signal, the magnetic field of the magnets must be very homogenous and a linear gradient field must be superimposed on it. However, it is extremely challenging to produce a field that has both a good field homogeneity and a reasonable field strength. This is why conventional MRI's use superconducting magnets. This design is very expensive and ultimately leads to a limited number of MRI scanners and therefore long MRI wait lists. Our solution is to use projection-based imaging. This unique approach relaxes the homogeneity constraints and removes the need for heavy gradient coils, thereby allowing our scanner to be cost-effective and lightweight.

1.2 Scope

The scope of this document is to outline the design specifications for each hardware and software component. The design considerations for each hardware and software component are presented. This document justifies the design choices chosen, focussing on the technical details and scientific background underlying the design choices, and cross-referencing the design choices with the functional requirements. Additionally, this document provides a template for any future modifications and testing procedures for the proof-of-concept model.

1.3 Intended Audience

This document is intended for use by all engineers at MRI Solutions. This document will be referred to by the engineers over the entire designing and construction phase. This document will also be useful for future engineers to take this project beyond the proof-of-concept stage. The test plan described in this document will be useful for evaluation and quality assurance.

2. System Design

The Portable MRI Scanner combines a magnet system, radiofrequency system, Field Programmable Gate Array (FPGA) control centre and a computer to produce detailed images of bone and soft-tissue. The system block diagram shown in Figure 2 provides an overview of the interaction and communication between each system.

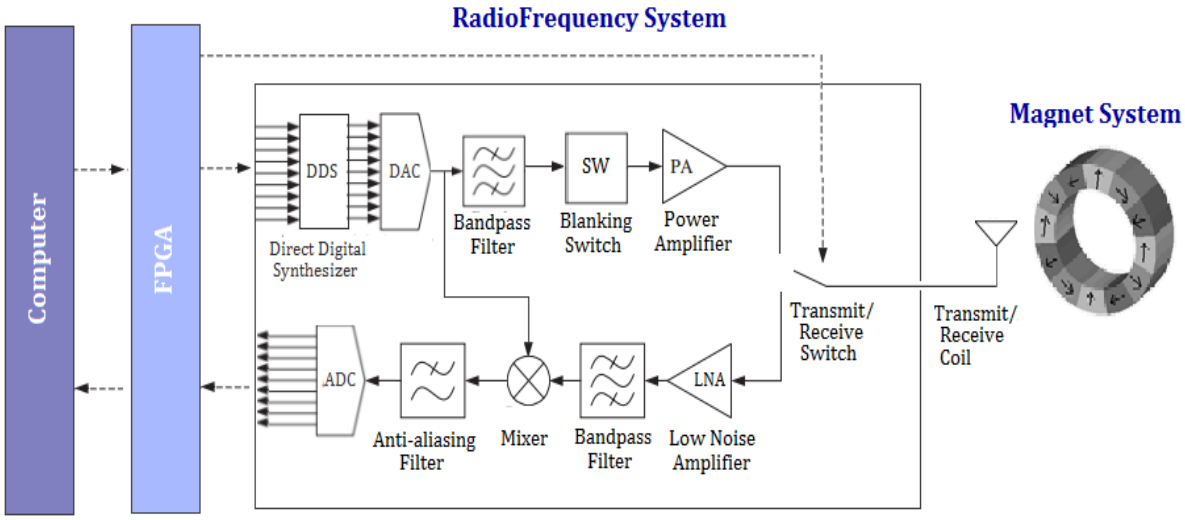

Figure 2: System Block Diagram

2.1 FPGA Control Centre

The FPGA is the "brain" of the prototype. It is the key element in coordinating the communication between different systems. The FPGA retrieves instructions from the user, decodes the instructions and sends appropriate commands to the radio frequency system. Its interaction with the radio frequency system includes crucial functions of programming pulse sequence, executing sampling, programming control signals and managing data flow.

2.2 Magnet System

The main purpose of the magnet system is to provide a strong external magnetic field such that hydrogen protons in the imaging sample precess or spin about an axis in the direction of the external magnetic field. The frequency of the precession is directly proportional to the strength of the magnetic field and this frequency is called the Larmor frequency. In order to transmit energy to the hydrogen protons, the RF coils must be tuned to the Larmor frequency.

2.3 Radio Frequency (RF) System

The RF system consists of a transmitter and receiver section. The transmitter performs the essential function of transmitting RF energy to hydrogen protons within the imaging sample. The hydrogen protons absorb the transmitted energy and the resulting additional energy causes a net magnetization in the transverse direction. As this net magnetization decays with time, an RF signal is emitted and the receiver is responsible for detecting this signal. This signal can be used to construct tissue contrast images.

2.4 Signal Processing System

The computer system provides a graphical user interface, allowing user to design and visually inspect pulse sequence. This instruction is passed to the FPGA. The computer system also streams data from the FPGA and performs signal processing to create tissue contrast images.

3. Magnet System

3.1 Magnet

3.1.1 Design Considerations

There are several magnets arrangements that can produce the strong (>0.1 T) and homogenous static magnetic field required for resonance purposes. One simple arrangement is the magnetic dipole, commonly configured in a C-shaped. However, this arrangement requires 2 very large neodymium magnets to produce a field of desired strength and homogeneity. Magnetic field produced by a dipole of length 8 inches and 2 inches thick is shown in Figure 3. In this case, the distance between dipoles is 2 inches. The size of the homogenous region will decrease when the distance between the magnets increases. To achieve a working space of 3 inches while maintaining a strong homogenous magnetic field, the magnets need to be 10-15 inches in length. The forces of attraction for magnets of this size are very strong and there is a lot of risk involved in handling large Neodymium magnets. Consideration must also be given to the yolk required to keep the magnets separated. The yolk needs to be very strong in order to handle the attraction forces of the magnets. As shown in the figure below, the dipole arrangement produces magnetic fields outside the magnet assembly. This stray magnetic field is undesirable as it poses safety concerns to people with electronic medical implants and it can also affect the radiofrequency components.

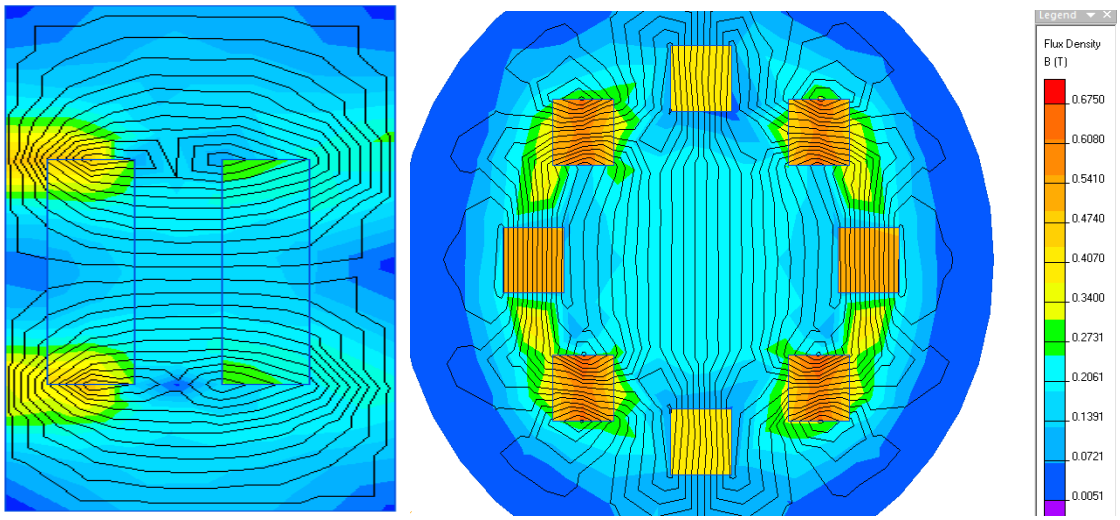

Figure 3: Magnetic field simulation for 8”x2” N42 magnets using QuickField (left) and magnetic field simulation for Halbach array using QuickField (right)

The Halbach arrangement provides an alternative solution. In a Halbach array, the magnets are arranged in spatially rotating pattern of magnetization. This particular arrangement augments the magnetic field on one side of the array while cancelling the field to near zero on the other side. The Halbach arrangement has the advantage of providing strong magnetic field and optimal homogeneity. In addition, the cylindrical Halbach arrangement allows the magnets to be easily rotated. This is critical for image reconstruction method that is based on a rotational spatial encoding field. The Halbach arrangement also does not produce stray magnetic field which satisfies requirement [MSR-3.2.4-I]. The magnetic field is produced in the radial direction inside the bore of the cylinder which meets requirement [MSR-3.2.3-I].

3.1.2 Magnet Design - Halbach Array

The magnetic field, B_o inside the Halbach cylindrical array is modelled by the equation

$$\mathrm{Bo} = \frac{n}{2}\,\mathrm{Br}\frac{R^2}{r^2}$$

where n is the number of cylinders, B_r is the remnant flux density, R is the radius of each cylinder and r is the distance between the center of the assembly and the center of the magnet piece. A higher magnetic field strength can be achieved by using more cylinders. But this significantly increases the cost of the magnets. Cylinder size is available in R = 0.56 inch and r is set to 2.75 inches to allow for sufficient working space. From the equation, 8 cylinders are sufficient to achieve a B_o that is greater than 0.1 T. This satisfies requirement [MSR-3.2.1-I] while keeping the budgetary cost affordable. The length of the magnets, L also affects B_o. When the ratio of L to r is equal to 2, the magnetic field inside the assembly is within 90% of the theoretical B_o and the actual B_o is at least 75% of the theoretical B_o [2]. Therefore, L must be equal to or greater than 2r.

Neodymium magnets are the strongest commercially available magnets. Grade N42 magnets were chosen because of their high magnetic remanence and manageable costs. Table 1, shows the specifications of magnet chosen for the Halbach array and the resulting static magnetic field strength. The magnet available is limited in size, so a cylinder is composed of three magnet pieces.

Table 1: Magnet specifications

Grade	Dimensions of one magnet piece (H x W x L)	Dimension of one cylinder (H x W x L)	B_r (T)	B_o(T)
N42	1" x 1" x 2"	1" x 1" x 6"	1.32	0.22

In Halbach array, the center of all magnets is located between the circumference of the inner and outer radii. As shown in Figure 4, the magnet position is defined by$\alpha$and the magnetization direction is defined by βaccording to the following equations

$$\alpha = 2\pi i/n$$

$$\beta = 2\alpha$$

where i = 0, 1, 2, .., n-1 and n is the number of cylinder.
Our Halbach array consists of 8 linear magnet arrays so $\alpha = \pi i/4$ and $\beta = \pi i/2$. This configuration results in each magnet array being placed at $\pi i/4$ interals and its magnetisation direction will be rotated by $\pi i/2$ at each interval. The inner diameter is 3 inches to allow sufficient working space and satisfying requirement [SR-2.4.2-I]. The detailed dimension of the arrangement is shown in Figure 4.

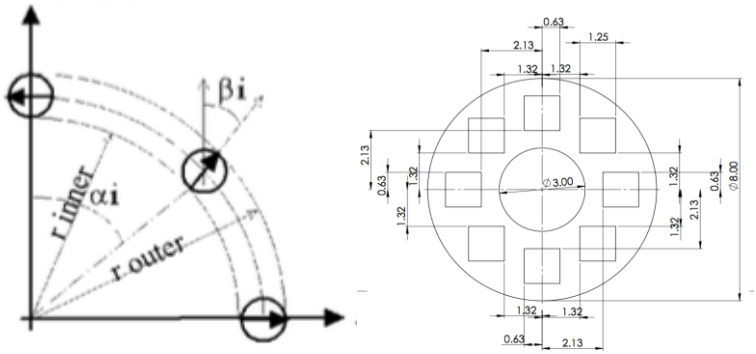

Figure 4: Halbach geometry [3] and dimensions

3.2 Magnet Housing

3.2.1 Magnet Housing Design

The mechanical housing must be non-magnetic and strong enough to overcome the pull-force between the individual magnet pieces. One housing option is to use 3D machined aluminium casing. This option is expensive and impractical when the manufacturing quantity is low. Another option is to use square tubes to hold the magnet pieces of each cylinder and a round frame to hold all the tubes or cylinders. A square fiberglass tube is chosen as the housing for each of the cylinders. The fibreglass can handle over 178 N pull-force which satisfies requirements [MSR-3.2.7-I] and [MSR-3.2.6-I]. Fibreglass is also the cheapest and lightest option that meets our requirements [MSR-3.2.7-I] and [SR-2.4.1-I] while also being a non-magnetic material which meets requirements [MSR-3.2.6-I]. Plywood is chosen as the round frame over plastics such as ABS because it is readily available in various thicknesses and is easy to shape into the desired dimensions. This option expedites the construction of proof-of-concept model. Future production will incorporate lightweight ABS frames instead of plywood. Consideration is also taken for recyclability of each material in order to meet requirements [SR-2.9.1-III] and [SR-2.9.2-III].

3.2.2 Magnet Housing Construction

To build a cylinder of 6” in length, three magnet pieces are glued using LePage epoxy (3200 psi) to satisfy requirement [MSR-3.2.8-I]. N42 magnets in linear arrays will produce strong repulsive forces, as a result, clamps are required to squeeze the magnets together and keep them in place long enough for the epoxy to cure (about 24 hours). To hold the 8 magnet arrays, ¾” plywood is chosen to fix the geometry and stabilize the housing structure meeting requirement [MSR-3.2.5-I]. The plywood pieces are cut precisely according to the calculated angles and desired radius of our Halbach array. Waterjet cutting is used to achieve high accuracy as the slightest misalignment could drastically change the resulting static magnetic field. Figure 5 shows the constructed frame.

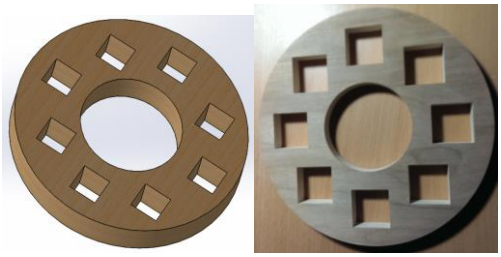

Figure 5: Plywood Frame

3.3 Field Mapping

3.3.1 Design Consideration

The use of a nonlinear magnetic field for image reconstruction means that prior knowledge of the field map is required. Thus, an accurate field mapping method is important. The magnetic field also needs to be measured whenever the magnet is relocated to a new location. This is because the field within the magnet system can be perturbed by external fields such as the earth's magnetic field. NMR probes are usually used for measuring inhomogeneous fields with high sensitivity [1]. However, NMR probes are not practical in our case as they require a working radio frequency transmitter and receiver. Future production may incorporate array of NMR probes for field mapping. A practical method for proof-of-concept is to use a linear Hall effect sensor that outputs a voltage proportional to the applied magnetic field. This method requires minimal hardware.

3.3.2 Field Mapping Design

An AD22151 magnetic field sensor is chosen because of its high sensitivity, adjustable gain, and linearity meeting requirement [MSR-3.3.2-I]. The Hall sensor produces a voltage offset in response to the perpendicular component of magnetic flux density. This voltage offset gives the magnitude of the magnetic field at that particular point. To accurately calculate the magnetic field strength at that particular point, the Hall effect sensor must be placed perpendicular to flux density. Since the magnetic field within the Halbach array is unidirectional, the AD22151 is configured to unipolar field sensing by using the layout shown in Figure 6.

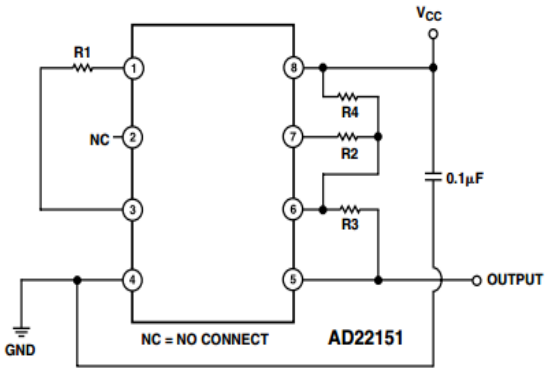

Figure 6: AD22151 in Unipolar Configuration [4]

A 22 kΩ R1 resistor is used to set the temperature compensation to +1200 ppm to counteract the inherent -1200 ppm temperature compensation of Neodymium magnets. To maximize output swing, the quiescent voltage (output voltage at zero magnetic field) is set to 1V. The sensitivity is set to 10mV/mT to provide a dynamic range of 0 to 350 mT within the linear output range [MSR-3.3.1-I]. A 120 kΩ R3 resistor is chosen to comply with current and power dissipation. The following equations are used to determine the R2 and R4 resistor values for the desired quiescent voltage and sensitivity.

$$Gain = 1 + \frac{R3}{R2||R4} \times 4mV/mT$$

$$R4 = \frac{R3}{\frac{V_{cc}/2 - V_{quiescent}}{V_{cc} - V_{quiescent}}} - R3$$

$$R2||R4 = \frac{R3}{Gain - 1}$$

Table 2: Design specifications for AD22151 magnetic field sensor

Specifications	Values
Sensitivity	10 mV/mT
Quiescent Voltage	1 V
Linear Output Range	0 - 350 mT
R1	22 kΩ
R2	109 kΩ
R3	120 kΩ
R4	300 kΩ

The output voltage of AD22151 is routed to a microcontroller (Arduino Uno) for analog to digital conversion and field calculation. Signal averaging technique is also used to improve signal-to-noise ratio (SNR).

3.4 Rotation Hardware

3.4.1 Design Consideration

The projection-based imaging method requires acquiring data at different projection angles. Thus magnetic field needs to be rotated around the imaging sample in fixed increments to collect spatial information at various angles. There are two ways to rotate the magnetic field. The ideal method is to place magnet cylinders horizontally on top of two rotating rods to spin the cylinders about a horizontal axis. This geometry is similar to that of conventional MRI and allows for imaging of different body parts. However, this method requires more complicated rotation hardware. To facilitate a fast proof-of-concept, we decided to rotate the magnetic field by placing the cylinder vertically and spinning it about a vertical axis. This rotation method requires only one rotating platform. Future production will incorporate horizontal rotation which allows for an easier method to stabilize and image different body parts.

3.4.2 Rotation Hardware Design

The array is mounted on a non-magnetic swivel plate so that it can be rotated with minimum friction meeting requirement [MSR-3.4.4-III]. Also, the rotation around vertical axis requires less force and the weight o.f the magnets will provide maximum stability which satisfy requirements [MSR-3.4.3-III] and [SR-

2.7.1-I]. It is also easier to measure the rotation angle and satisfy requirement [MSR-3.4.1-I] in this configuration. The transmitting coil is mounted on stationary platform and the whole assembly is shown in Figure 7. The sample will be placed inside the stationary solenoid while the magnetic field rotates around the sample.

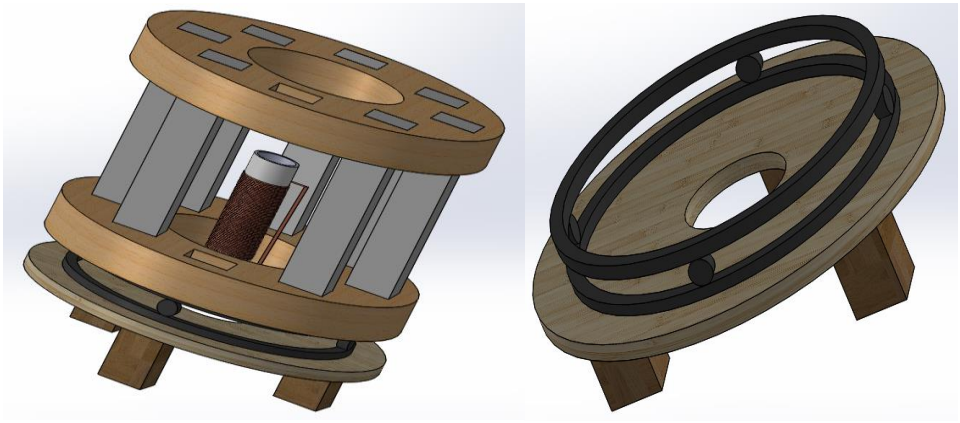

Figure 7: Overall housing assembly (left) and Swivel plate for rotation (right)

4. Radio Frequency System

4.1 Direct Digital Synthesizer (DDS) and Digital-to-Analog Converter (DAC)

Direct Digital Synthesis is a method of producing analog waveforms by generating a time-varying signal in digital form and then performing a digital-to-analog conversion [5]. Alternatively, a sine wave can be generated by implementing a digital phase-locked loop on the FPGA and then performing digital-to-analog conversion. However, this method requires additional programming which is not feasible given our limited time constraint.

The constructed magnet system produces a measured field of 0.25 T which corresponds to a Larmor frequency

$$f_0 = \frac{\gamma B_{max}}{2\pi} \qquad \text{where } \frac{\gamma}{2\pi} \text{ is gyromagnetic ratio (Hydrogen= 42.5 MHz T}^{-1}\text{)}$$

of 10.6 MHz. The AD9954 DDS from Analog Devices is chosen because it can generate sine waves at this frequency accurately and meets requirements [RFR-4.2.1-I] & [RFR-4.2.2-I].

The AD9954 is programmed through a high speed serial peripheral interface (SPI), and requires only an external clock to generate sine waves. The functional blocks inside the AD9954 DDS system are: Phase Register, Phase-to-Amplitude Converter, and Digital-to-Analog Converter. The phase register along with a summing junction equates to the phase accumulator. The main input for the phase accumulator is a 32-bit frequency tuning word. The 32 bit tuning word is programmed into the FPGA board and is passed through I/O port of DDS. Along with the external 10Mhz clock, the phase accumulator computes the corresponding phase from the sine look-up-table, and subsequently outputs the digital value of the amplitude. The Digital-to-Analog converts the digital value of the amplitude to a corresponding analog voltage or current.

Table 3: Design specifications for AD9954/PCBZ Direct Digital Synthesizer

Specifications	Values
Direct Digital Synthesizer Model	AD9954/PCBZ
I/O Port	High Speed Serial (Centronics DB-36)
Digital-to-Analog Converter	14 Bits
RF Output Channels	2 Channels
Tuning Word	32 Bits
Internal Clock Speed	400 MSPS

4.2 Bandpass Filter

A 5th order Butterworth bandpass filter, shown in Figure 8, is designed to selectively pass the Larmor frequency bandwidth [RFR-4.2.3-I]. A Butterworth filter is chosen because of its flat passband and a 5th order filter is chosen for steeper power rolloff as the slope is defined by $20n$ dB/decade where n is the

order of the filter. The bandpass filter can be built on copper clad board for simplicity and the large grounding plane provides additional RF shielding.

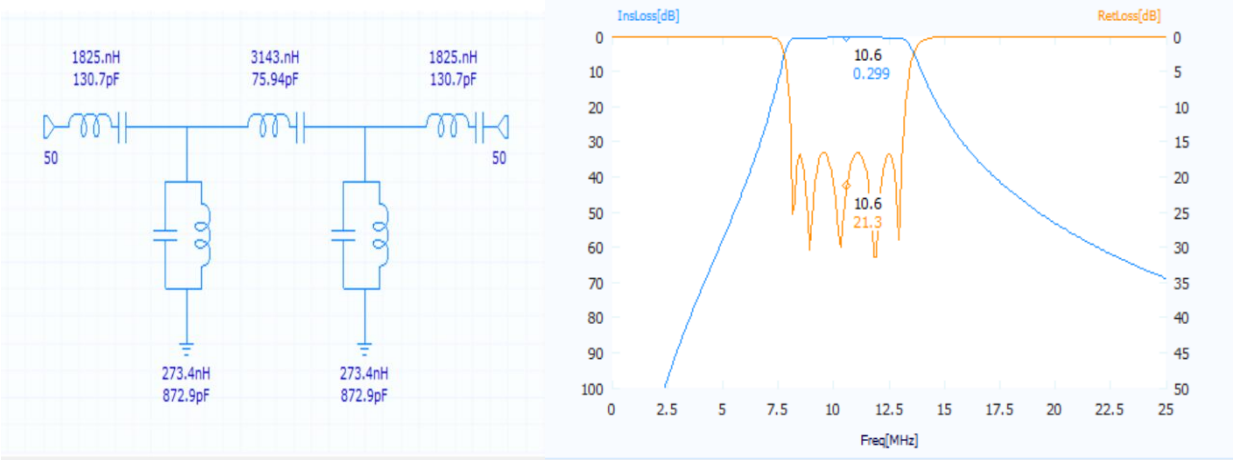

Figure 8: Bandpass filter design (left) and simulated frequency response (right) in AWR Software

4.3 Blanking Switch

A blanking switch is needed to blank the input to the power amplifier between RF pulses. Although a switch can be built using PIN diodes, purchasing a switch guarantees safe and high isolation. A ZX80-DR230+ Single Pole Double Throw (SPDT) absorptive switch from Mini-Circuits is chosen because it provides 2 µs switching time, 0.7 dB low insertion loss and 50 Ω high isolation from DC to 3000 MHz operating frequency. These specifications satisfy the requirements [RFR-4.2.5-I], [RFR-4.2.8-I] and [RFR-4.2.6-I]. Figure 9 shows the pin configuration and Table 4 provides the pin description. The switch can be controlled via two GPIO pins on the FPGA. The truth table is provided in Table 5.

Table 4: Blanking Switch Pin Descriptions

Function	Pin	Descriptions
RF2	J1	Input to power amplifier
RF COM	J2	Output from bandpass filter
RF1	J3	Open
Control 1	P1	GPIO Pin on FPGA [PIN_A13]
GND	P2	Ground
Control 2	P3	GPIO Pin on FPGA [PIN_A14]
GND	P4	Ground
VDD	P5	5 V supply voltage [PIN_B11]

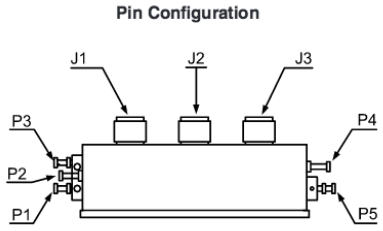

Figure 9: ZX80-DR230+ Pin Configuration

Table 5: Blanking Switch Truth Table

Control 1	Control 2	State
Low	High	ON (amplify input)
High	Low	OFF (blank input)

4.4 Power Amplifier

The power requirement depends on the magnetic field required to tip protons by an angle ϕ which is determined by

$$B_1 = \frac{\phi}{2\pi\gamma T}$$

where T is the pulse length. A longer T means that a smaller B_1 is required to tip the precessing protons. The problem is protons grow out of phase quickly in an inhomogeneous field and this can result in zero net magnetization. Therefore, a short T and large B_1 is necessary. At 10.6 MHz, the protons are precessing at 0.0943 µs. As shown in Figure 10, A 5 µs period (T) is chosen to minimize B_1 while keeping phase difference well below 1 revolution.

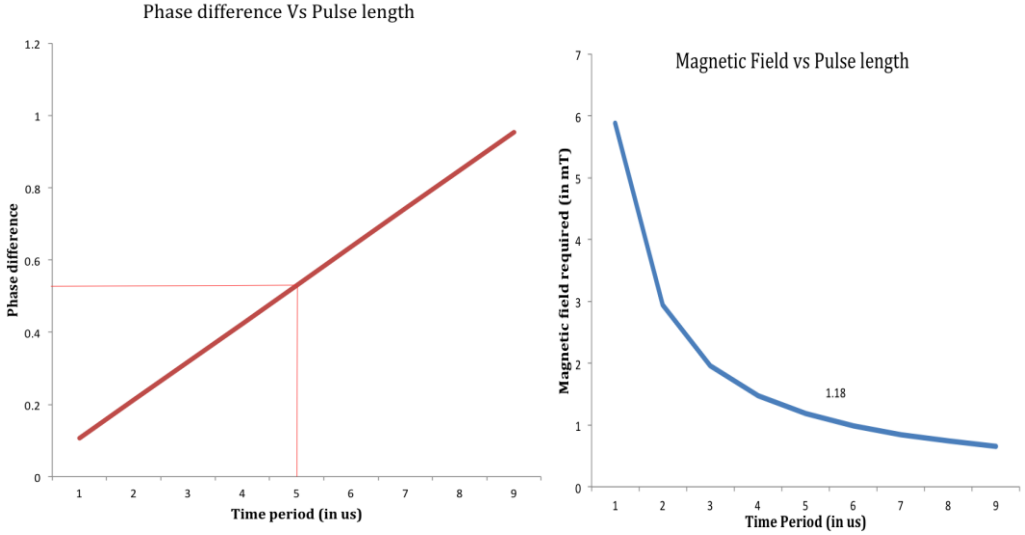

Figure 10: Phase difference (left) and Magnetic field vs Pulse length (right)

Using a 5 µs period, B_1 is 1.176 mT. In order to generate this magnetic field, the current required to drive a tightly wound inductor, I is

$$I = B_1 \frac{d}{\mu_0}$$

where *d* is the diameter of the wire and μ_o is the vacuum permeability. Figure 11 shows the range of current and power required to generate a B_1 of 1.176 mT depending on the diameter of wire used.

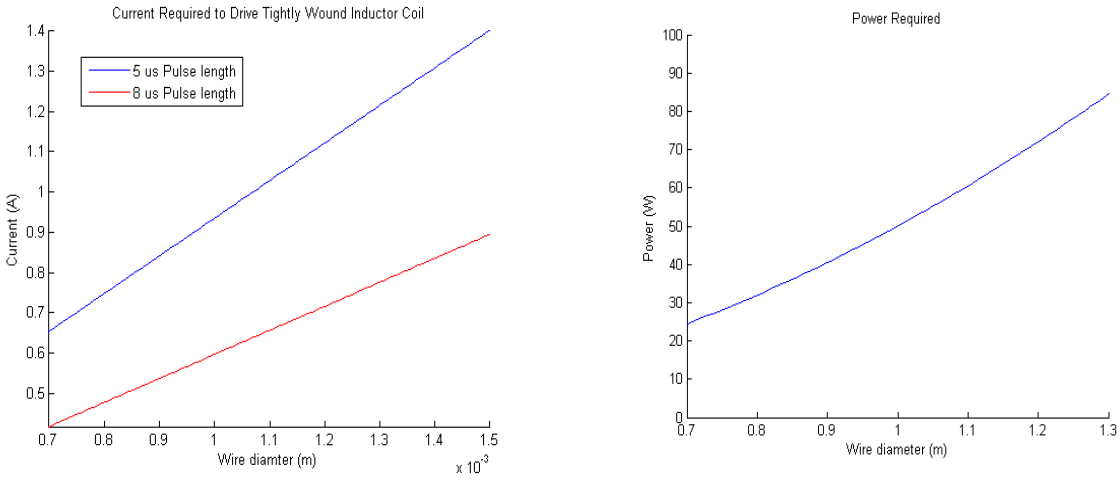

Figure 11: Current requirement (left) and Power requirement (right)

New Henry T100 Series 100 Watt power amplifier is selected because it is the cheapest option and it satisfies the cost and power requirements [SR-2.5.5-I] and [RFR-4.2.4-I]. Most power amplifiers are in the price range of $10,000 to $15,000. Building a power amplifier is most certainly out of the scope of this project. Note that this is a continuous power amplifier so a blanking switch is required.

4.5 Transmit/Receive (T/R) Coil

The system requires a coil in close proximity to the sample, in order to provide sufficient energy to the protons in the sample [RFR-4.2.7.I]. For the proof-of-concept, the same coil will be used to monitor the response of the signal.

4.5.1 Coil Design

The T/R coil needs to resonate at the Larmor frequency. Considering an inhomogeneous field, the T/R coil also needs to cover the encoding bandwidth such that the same tip angle is applied to the entire imaging region. This means that an inductor of low quality factor, Q, is required to cover the wider bandwidth. Q is determined by

$$Q=\frac{2\pi fL}{r}$$

where L denotes the inductance and r denotes the resistor in series with the inductor. High r is undesirable because it causes unwanted power dissipation and a heating effect. Therefore, a low L is preferred to achieve a low Q. Inductance of the coil, in μH, is given by

$$L=\frac{0.394N^2r^2}{(9r+10l)}$$

where *r* is the radius of coil (cm), *l* is the inductor length (cm) and *N* is the number of turns.

The length of wire used to construct the solenoid is limited by stray capacitance. Stray capacitance can be ignored if the length of wire is smaller than ¼ of the wavelength at Larmor frequency. Since 10.6 MHz corresponds to about λ =28 m, the length of wire cannot exceed 7 m. AWG 23 wire (0.57mm diameter) is chosen to maximize the number of turns made by tightly winding this wire on a plastic pipe with outer diameter of 1.05". The wire has a current rating of 4.7 A which satisfies requirement [SR-2.5.2-I]. To keep the inductance low, 40 turns are chosen which results in a length of 2.28 cm for the inductor. The inductance is calculated to be 31 µH. For Q = 50, the value of r is 41 Ω. Using AWG 23 wire, 0.53 A current is needed to generate the B_1 magnetic field required. These design choices satisfy requirement [RFR-4.2.14-I].

4.5.2 Matching and Tuning Circuit

To ensure that maximum power is delivered to the T/R coil, an additional circuit is required to match the impedance of the T/R coil to the 50 Ω output impedance of the power amplifier. Instead of placing the matching and tuning circuit within the magnet system, the circuit will be placed far away from the magnets. This approach allows for remote tuning which is important since introducing sample in the T/R coil can introduce capacitive coupling which affects the inductance of the coil at the Larmor frequency. This also eliminates the need for more expensive non-magnetic components and it satisfies requirement [SR-2.5.3-I].

A capacitive matching and tuning circuit is chosen over an inductive circuit because capacitors are available in a wide range of values. As shown in Figure 12, the circuit consists of a variable tuning capacitor (C_T) and a matching capacitor (C_M).

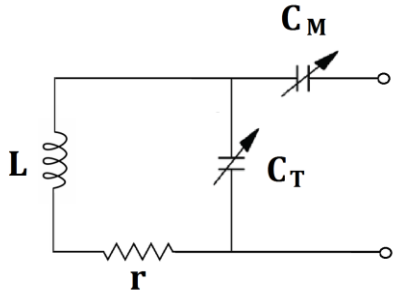

Figure 12: Tuning and matching circuit

The values of C_T and C_M can be calculated using the following equations,

$$C_T = \frac{Q-A}{\omega B} \text{ and } C_M = \frac{1}{\omega B Z}$$

where Z = 50, $A = \sqrt{\frac{B}{Z} - 1}$ and $B = r\,(1+Q^2)$ [6]. For a frequency of 10.6 MHz, C_T = 0.693 pF and C_M= 6.63 pF. This circuit can be built on a copper clad board to keep the designing process simple and economical. Also, this board provides a convenient ground for the components meeting requirement [SR-2.7.6-I]. Note that addition of C_T and C_M is equal to the resonant capacitance $C = \frac{1}{\sqrt{\omega L^2}}$. Figure 13 shows that the calculated capacitance indeed tunes the circuit to 10.6 MHz and matches the circuit to 50 Ω.

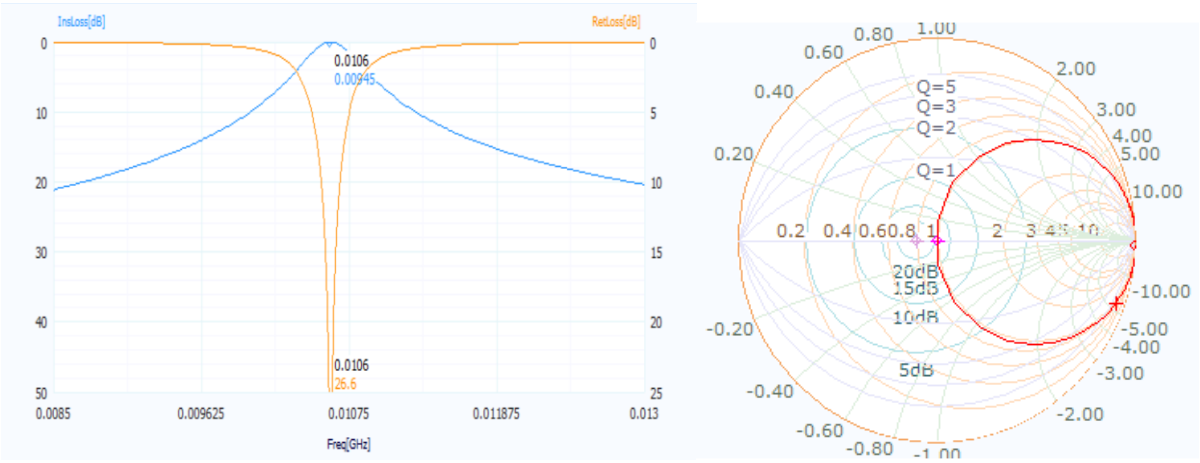

Figure 13: Frequency Response (left) and Smith Chart showing impedance matching(right)

4.6 Transmit/Receive Switch

The T/R switch is incorporated to protect the receiving circuit from the high power transmitting circuit. Similar to the blanking switch in Section 4.3, ZX80-DR230+ absorptive switch from Mini-Circuits is chosen. Table 6 and 7 show the change in pin configurations and truth table.

Table 6: Transmit/Receive Switch Pin Description

Function	Pin	Descriptions
RF2	J1	Input to low noise amplifier
RF COM	J2	T/R coil
RF1	J3	Output from power amplifier

Table 7: Transmit/Receive Switch Truth Table

Control 1	Control 2	State
High	Low	Transmitting
Low	High	Receiving

4.7 Low Noise Amplifier

The receiving signal is generally very weak. It is important to amplify the signals without adding excessive distortion. The GALI-74+ monolithic amplifier is chosen because of its high 25.1 dB gain, low 2.7 dB noise figure, 50 Ω matched impedance and wide operating frequency of up to 1 GHz. The bias resistor value is calculated based on the required 80 mA bias current I_{bias}, 4.8 V typical operating voltage V_d and 5V V_{cc} according to the equation $I_{bias} = (V_{cc} - V_d)/R$. To achieve 50 dB gain, two Gali-74+ are cascaded as shown in Figure 14. Although this does not satisfy requirement [RFR-4.2.9-I], it is deemed that 50 dB gain and 2.7 dB

noise figure are acceptable and the original requirement has been set too high for proof-of-concept purposes.

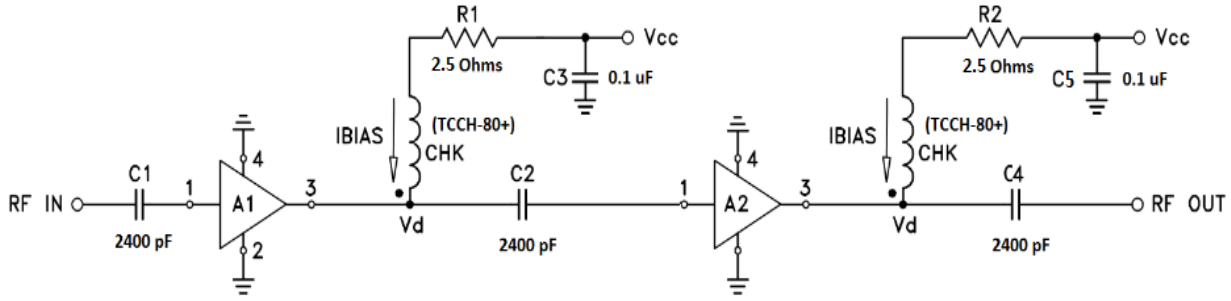

Figure 14: Cascaded low noise amplifier

4.8 Mixer

As shown in figure 15, the frequency mixer is a three port nonlinear device that performs downconversion to allow high frequency signals to be sampled by a subsequent Analog-to-Digital (ADC) converter. There are many downconversion strategies and the zero-IF (Intermediate Frequency) downconversion is a simple method. In the zero-IF downconversion method, the transmitted carrier frequency is used as local oscillator (LO) to produce a downconverted IF signal centered at 0 Hz. An ADE-1+ mixer from Mini-Circuits is chosen because it has a low 5 dB conversion loss which satisfies requirement [RFR-4.2.10-I]. Note that a mixer is no longer included in the proof-of-concept model because the ADC described in Section 4.11 has a sample rate of up to 65 MHz. Therefore, frequencies less than 30 MHz can be sampled directly. This is desirable as it avoids nonlinear mixing effects that may be introduced by the mixer. Final production will include the chosen ADE-1+ mixer to allow sampling of higher frequencies.

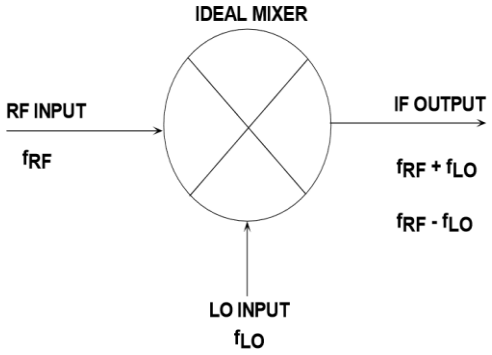

Figure 15: Frequency Mixer [7]

4.9 Anti-Aliasing Filter

Frequencies that exceed the Nyquist frequency are aliased and indistinguishable. The anti-aliasing filter removes these high frequency signals so that they are not digitized by the ADC. Anti-aliasing filter is essentially low pass filter which can be easily designed and constructed on copper clad board or incorporated on the printed circuit board (PCB) for the ADC. In proof-of-concept model, these high frequency signals are removed by the bandpass filter. An Anti-aliasing filter is therefore not included. In the final production model, the addition of a mixer may introduce frequencies that exceed the Nyquist frequency so anti-aliasing filter must be incorporated to satisfy requirement [RFR-4.2.11-I].

4.10 Analog-to-Digital Converter

The received analog signal needs to be digitized prior to signal processing. As the highest frequency of the filtered signal is around 10.6 MHz, a minimum sampling rate of 21.6 MHz is required. AD9244 from Analog Devices is chosen because it provides 14-bit resolution and 65 MSPS throughput rate which satisfies requirements [RFR-4.2.13-I] and [RFR-4.2.12-I]. The high sampling rate of AD9244 allows frequencies lower than 30 MHz to be sampled directly. This simplifies the sampling hardware required for the proof-of-concept model. This ADC can also be used for future production provided that a mixer and anti-aliasing filter are incorporated.

5. Software System

The Field Programmable Gate Array board is essentially the control center for the communication between different systems. The Field Programmable Gate Array used for our portable MRI Scanner is the Altera DE-1 board, it is compact in terms of size which satisfies the requirement [FP-6.2.4-I]. The specifications of the FPGA board is shown in Table 8. The Altera DE-1 FPGA board is chosen mainly because of the 50 MHz oscillator clock source and the expansion headers (GPIO - General Purpose Input/Output) providing up to 76 pins [FP-6.2.1-I]. The 50MHz oscillator crystal clock source provides sufficient clock speed for the requirement [FP-6.2.2-I]. The serial RS-232 port serves as the connection bridge between FPGA and DDS satisfying requirement [FP-6.2.10-I].

5.1 FPGA Programming

The FPGA board will be programmed as an embedded system using the onboard Nios II Processor. Between the embedded system on the FPGA board and the DDS, the UART core with Avalon interface allows the communication to occur, by implementing RS-232 protocol timing, and provides an adjustable baud rate and data bits. The data bits transmitted are the spin echo pulse in digital values.

Table 8: Altera DE 1 Field Programmable Gate Array Specifications

Altera DE 1 FPGA	Values
Operating Voltage	7.5V
Input Voltage	7.5V
Clock Speeds	50Mhz, 27Mhz, 24Mhz **1
Expansion Headers (GPIO)	76 Pins **2
SRAM	8 MB
Flash Memory	4 MB
Pushbutton Switches	4 Total **3
Serial Port	RS-232 (DB-9 Serial Connector)

****1 - Clock Speeds [FP-6.2.2-I], **2 - Expansion Headers (GPIO) [FP-6.2.3-I], **3 - Pushbutton Switches [FP-6.2.7-I]**

The embedded system will control the Blanking switch and Transmit/Receive switch which is dependant on the timing of transmitting and receiving radiofrequency signals, and the communication of the spin echo pulse to our Direct Digital Synthesizer. The system will initialize the DDS, by calculating the necessary tuning word to stream the spin echo pulse towards the DDS. This relationship is found from the basic tuning equation for DDS architecture:

$$f_{\text{out}} = \frac{MxfC}{2^{32}}$$

where: f_{out} = output frequency in DDS, M = binary tuning word, f_C = internal reference clock frequency (system clock), *32* = length of the phase accumulator (AD9954), in bits. The system will contain the necessary interrupts in order to allow for testing purposes and modular design.

6. System Test Plan

As the proof-of-concept MRI scanner is envisioned to be a medical device, the MRI scanner will be tested rigorously to ensure we can provide users and operators with a safe, reliable and high quality product. Testing will begin with individual component testing, followed by testing of each module, and completed by testing the entire system as a whole.

6.1 Halbach Array Testing

1. Halbach array will be tested by inspecting the stability of the housing and comparing it with the requirements of [MSR-3.2.5-I] and [MSR-3.2.7-I].
2. Magnetic field strength in the center of the magnet assembly will be measured with a Hall effect sensor to ensure that requirement [MSR-3.2.1-I] is met or exceeded.
3. A field map will be created using the same Hall effect sensor in the 3 inch opening to meet the requirements of [MSR-3.2.2-I] and [MSR-3.2.4-I].

6.2 RF Transmitting Module Testing

1. The sine wave output from the DDS will be tested using an oscilloscope to ensure that the signal is oscillating at the correct frequency.
2. The bandpass filter will be tested using an oscilloscope to measure the frequency response and ensure that requirement [RFR-4.2.3-I] is met.
3. The output signal from the power amplifier will be tested using an oscilloscope to measure the gain and ensure that requirement [RFR-4.2.4-I] is met.
4. The blanking switch and transmit/receive switch will be tested in conjunction with the FPGA using an oscilloscope to ensure correct pulsing.
5. Inductance of the coil will be measured using a LRC bridge (Tedam/ESI LRC Bridge 2400).
6. The tuning circuit will be tested using a function generator and oscilloscope to check if the coil is tuned to Larmor Frequency.
7. The matching circut will be tested using a Digital Multimeter to make sure that the impedance is matched to 50Ω.

6.3 RF Receiving Module Testing

1. The output signal from LNA will be tested using an oscilloscope and function generator to make sure that the signal is amplified by 50 dB.
2. The output of the bandpass filter will be tested by using an oscilloscope to make sure the signal passed is centred at the Larmor Frequency and requirement [RFR-4.2.3-I] is met.
3. The output of ADC will be tested by passing a known signal to the FPGA through the ADC and checking that the digitized signal is valid.

6.4 FPGA Module Testing

1. The FPGA and DDS connection will be tested through a series of simulations ensuring the data streamed onto the DDS can be read [FP-6.2.10-I].

2. The expansion header pins for the transmit/receive switch and blanking switch will be tested using oscilloscope to check the validity of switch programming.
3. The ADC and FPGA connection will be tested through a series of simulations ensuring the 14-bit data will be eventuated onto our computer.

6.5 Overall System Testing

Pending successful testing of magnet system, transmission and receiving module. Overall system will be tested by placing a sample inside the transmitting coil. The transmission line is expected to produce an oscillating magnetic field through the coil. The response from the sample is captured by the same coil, sent back to the FPGA through receiving module and displayed on a computer.

7. Conclusion

This document outlines the design specifications for the portable low cost MRI scanner. Justifications for the chosen design approach is given with additional focus on the technical details and scientific background underlying the design choices. Included is a detailed test plan with corresponding requirements from the function specifications as well as detailed functioning of each component of our product. As the project progresses, this document will serve as a guideline to ensure that we are able to achieve the highest quality and reliability of our product.

8. References

[1] C. Zimmerman Cooley, 'Portable Low-cost Magnetic Resonance Imaging', 2014. [Accessed: 10- Nov- 2015].

[2] B. Zhang and G.P. Hatch. Field analysis and comparison of several permanent magnet dipole structures. IEEE Trans. Magn., 45(10): 4395-4398, October 2009

[3] P. Poulichet, A. Fakri and C. Delabie, 'Simulation and optimisation of homogeneous permanent magnet for portable NMR applications' , Proceedings of the 8th International Conference on Sensing Technology, 2014

[4] www.analog.com, 'AD22151 Linear Output Magnetic Field Sensor Datasheet', 2015. [Online]. Available: http://www.analog.com/media/en/technical-documentation/data-sheets/AD22151.pdf. [Accessed: 11- Nov- 2015].

[5] www.analog.com, 'ADI - Analog Dialogue | Direct Digital Synthesis (DDS)', 2015. [Online]. Available: http://www.analog.com/library/analogDialogue/archives/38-08/dds.html. [Accessed: 10- Nov- 2015].

[6] J. Mispelter, M. Lupu and A. Briguet, *NMR probeheads for biophysical and biomedical experiments*. London: Imperial College Press, 2006.

[7] Analog.com, 'Analog-Dialogue | Volume 43, 2009 [Online]. Available: http://www.analog.com/library/analogDialogue/archives/43-09/EDCh%204%20rf%20if.pdf.[Accessed: 10- Nov- 2015].